

<sup>1</sup> **Mediterranean drought variability over the last millennium**

<sup>2</sup> Benjamin I Cook<sup>1,2</sup>, Kevin J Anchukaitis<sup>3,4,5,6</sup>, Ramzi Touchan<sup>4</sup>, David M

Meko<sup>4</sup>, and Edward R Cook<sup>6</sup>

Corresponding author: Benjamin I Cook, NASA Goddard Institute for Space Studies, New York, New York, USA. (benjamin.i.cook@nasa.gov)

<sup>1</sup>NASA Goddard Institute for Space Studies, New York, New York, USA.

<sup>2</sup>Ocean and Climate Physics,  
Lamont-Doherty Earth Observatory,  
Palisades, New York, USA.

<sup>3</sup>School of Geography and Development,  
University of Arizona, Tucson, Arizona,  
USA.

<sup>4</sup>Laboratory of Tree-Ring Research,  
University of Arizona, Tucson, Arizona,  
USA.

<sup>5</sup>Woods Hole Oceanographic Institution,  
Woods Hole, Massachusetts, USA.

<sup>6</sup>Tree Ring Laboratory, Lamont-Doherty  
Earth Observatory, Palisades, New York,  
USA.

**Abstract.** Recent droughts in the Mediterranean have highlighted concerns that anthropogenic climate change may be contributing to observed drying trends, but the full range of natural climate variability in the region is still poorly understood. Here, we analyze 900 years (1100–2012) of Mediterranean drought variability in the Old World Drought Atlas (OWDA), a spatiotemporal tree-ring based reconstruction of the June–July–August self calibrating Palmer Drought Severity Index. In the Mediterranean, the OWDA is highly correlated with spring precipitation (April–June), the North Atlantic Oscillation (January–April), the Scandinavian Pattern (January–March), and the East Atlantic Pattern (April–June). Drought variability in the basin shows significant east-west coherence on multi-decadal to centennial time scales, contrary to previous analyses. We also find significant North-South antiphasing in the eastern Mediterranean, with a tendency for the Black Sea region (e.g., Greece, Anatolia, the Balkans, etc) to be wet when coastal Libya, the southern Levant, and the Middle East are dry, possibly related to variability in the North Atlantic Oscillation. Recent droughts are centered in the western Mediterranean, Greece, and the Levant region. Events of similar magnitude in the western Mediterranean and Greece are apparent in the OWDA back to 1100 CE, but the most recent 15-year drought in the Levant (1998–2012) appears as the driest such period in the record. Estimating sampling uncertainties using a Monte-Carlo approach, we conclude there is an 89% likelihood that the recent Levant drought is drier than any comparable pe-

<sup>25</sup> riod of the last 900 years, possibly indicating the emergence of an anthro-  
<sup>26</sup> pogenically forced drying signal.

## 1. Introduction

27 Climate change impacts on water resources are a significant concern in the regions sur-  
28 rounding the Mediterranean Sea [Iglesias *et al.*, 2007; García-Ruiz *et al.*, 2011], an area  
29 including southern Europe, Northern Africa, and the Levant (Cyprus, Israel, Jordan,  
30 Lebanon, Palestine, Syria, Turkey) region of the Middle East. Projections from climate  
31 models almost uniformly point towards drying in the Mediterranean from increased green-  
32 house gas forcing in the coming decades [Giorgi and Lionello, 2008; Collins *et al.*, 2013;  
33 Seager *et al.*, 2014], part of an overall trend towards desiccation and poleward expansion  
34 of subtropical dry zones [Held and Soden, 2006; Seager *et al.*, 2010]. Indeed, analyses  
35 of recent climate trends in the region suggest that this process may have already begun  
36 [García-Ruiz *et al.*, 2011; Gleick, 2014; Hoerling *et al.*, 2012; Kelley *et al.*, 2012, 2015].

37 However, a more complete understanding of natural Mediterranean drought variability  
38 and anthropogenically forced moisture trends requires comparisons with long-term vari-  
39 ability that is not available from relatively short instrumental records. To this end, the  
40 paleoclimate community has been active throughout this region, developing estimates of  
41 Common Era drought variability from a variety of proxies, including tree-rings [Chbouki  
42 *et al.*, 1995; Glueck and Stockton, 2001; Touchan *et al.*, 2003; Akkemik and Aras, 2005;  
43 Touchan *et al.*, 2005; Esper *et al.*, 2007; Andreu *et al.*, 2007; Nicault *et al.*, 2008; Touchan  
44 *et al.*, 2008a; Büntgen *et al.*, 2010; Touchan *et al.*, 2011; Köse *et al.*, 2011; Touchan *et al.*,  
45 2014a], sediment cores [e.g., Jones *et al.*, 2006; Roberts *et al.*, 2012; Moreno *et al.*, 2012],  
46 and speleothems [e.g., Jex *et al.*, 2011; Wassenburg *et al.*, 2013]. To date, however, there is  
47 little consensus across these different records regarding the character and dominant drivers

of drought variability across the basin over the last millennium. In particular, there are extant uncertainties regarding how widespread droughts are in the Mediterranean [Roberts *et al.*, 2012], the magnitude and timing of long-term trends and centennial-scale variability [Esper *et al.*, 2007; Touchan *et al.*, 2011; Wassenburg *et al.*, 2013], and how seasonal signals and large-scale climate modes are reflected in proxy reconstructions [Touchan *et al.*, 2014a, b; Seim *et al.*, 2014].

Given these uncertainties, the development and analyses of new large-scale reconstructions is imperative for improving our understanding of regional climate dynamics in the Mediterranean region. Here, we use a spatially resolved tree-ring based field reconstruction of European and Mediterranean drought to investigate the dominant spatial and temporal patterns of drought variability across the basin over the last millennium. Specifically, our analysis addresses three primary research questions: 1) What are the dominant modes of hydroclimate variability in the Mediterranean? 2) How spatially coherent are drought events across the Mediterranean basin? and 3) How do recent droughts compare to long-term hydroclimate variability over the last millennium?

## 2. Materials and Methods

### 2.1. The Old World Drought Atlas

The Old World Drought Atlas [OWDA; Cook *et al.*, in revision] is a new, tree-ring based reconstruction of summer season (June-July-August, JJA) self calibrating Palmer Drought Severity Index (scPDSI) [van der Schrier *et al.*, 2013]. The OWDA uses 106 tree-ring chronologies to reconstruct scPDSI at 5,414 half degree grid points for the entire Common Era over the European-Mediterranean domain ( $27^{\circ}\text{N}$ – $71^{\circ}\text{N}$ ,  $12^{\circ}\text{W}$ – $45^{\circ}\text{E}$ ). The reconstruction uses the point-by-point method [Cook *et al.*, 1999, 2013] with a search radius of 1000

69 kilometers around each target grid point. Grid cell scPDSI is reconstructed from the proxy  
70 predictor series within the search radius, but the tree-ring proxies are effectively weighted  
71 by the principal components regression such that those that covary most strongly with  
72 observations have the greatest influence on the reconstructions. Proxy site locations in  
73 the Mediterranean portion of the OWDA ( $30^{\circ}\text{N}$ – $47^{\circ}\text{N}$ ,  $10^{\circ}\text{W}$ – $45^{\circ}\text{E}$ ) are shown in Figure  
74 1, along with the approximate start date of the various records. We restrict our analy-  
75 sis to 1100–2012 CE, the interval during which the Mediterranean domain is reasonably  
76 well sampled by proxy sites. Values in the OWDA through 1978 are reconstructed from  
77 tree-ring chronologies, while from 1979–2012 the OWDA incorporates the instrumental  
78 scPDSI.

79 The scPDSI is a modification of the original PDSI formulation of *Palmer* [1965], a  
80 locally normalized drought index incorporating changes in supply (precipitation), demand  
81 (evapotranspiration), and storage (soil moisture). PDSI has an inherent memory timescale  
82 of 12–18 months [*Guttmann*, 1998; *Vicente-Serrano et al.*, 2010], allowing the JJA target of  
83 the OWDA to incorporate climate information from the previous winter and spring, the  
84 main seasons of moisture supply to the Mediterranean. The scPDSI used as the target for  
85 the OWDA reconstruction [*van der Schrier et al.*, 2013] is calculated from version TS3.21  
86 of the high-resolution CRU climate grids [*Harris et al.*, 2014], incorporates a snow module,  
87 and uses the Penman-Monteith formulation for calculating potential evapotranspiration  
88 [*Xu and Singh*, 2002]. .

## 2.2. Climate Data

89 Monthly precipitation data used in the analyses are from the high-resolution CRU gridded  
90 climate data [TS3.21, *Harris et al.*, 2014]. We also use monthly average indices from the

91 Climate Prediction Center from climate modes previously shown to have an influence on  
92 Mediterranean climate [Sousa *et al.*, 2011]. The North Atlantic Oscillation [NAO; Hurrell,  
93 1995] consists of a north-south dipole in atmospheric pressure between Greenland and the  
94 subtropical North Atlantic, with positive phases typically associated with below-average  
95 precipitation in the Mediterranean and southern Europe. The Scandinavian Pattern [SCA;  
96 Bueh and Nakamura, 2007] is centered over Scandinavia, with positive height anomalies in  
97 this region causing above-average precipitation across central and southern Europe. The  
98 East Atlantic Pattern [EA; Barnston and Livezey, 1987] is similar to the NAO, consisting  
99 of a north-south anomaly dipole in the Atlantic. Unlike the NAO, however, the EA has  
100 stronger connections to the subtropical ridge. Positive phases of the EA are linked to  
101 below average precipitation across southern Europe. For the CRU precipitation data and  
102 the climate indices, we restrict our analysis for the most recent period when data quality  
103 and availability is highest (1950–2012).

### 2.3. Analyses

104 We use Spearman's rank correlations to assess the statistical relationship between recon-  
105 structions, observations, and indices. Spearman's is a non-parametric alternative to the  
106 Pearson product-moment correlation that is less sensitive to outliers. We also conduct  
107 spectral and spectral coherency analyses using a multi-taper approach [Thomson, 1982;  
108 Chave *et al.*, 1987; Mann and Lees, 1996; Czaja and Marshall, 2001; Huybers, 2004] with  
109 significance levels estimated using a non-parametric Monte Carlo procedure with red noise  
110 (AR1) conditioned on the original data. We also use wavelet coherency analyses [Maraun  
111 and Kurths, 2004; Maraun *et al.*, 2007] to investigate time-varying coherency and phase  
112 between various drought series. In some figures, the time series were smoothed using

<sup>113</sup> a 10-year loess fit [*Cleveland and Devlin, 1988*] to emphasize low frequency variability,  
<sup>114</sup> although all statistical analyses were conducted on the original (unfiltered) data.

### 3. Results

#### 3.1. Climate Signals in the OWDA

<sup>115</sup> Correlations between winter (January–March; JFM) and spring (April–June) precipita-  
<sup>116</sup> tion and the tree-ring reconstructed JJA scPDSI are uniformly positive across the basin  
<sup>117</sup> (Figure 2). The strongest correlations with JFM precipitation are localized in Spain and  
<sup>118</sup> Morocco in the western Mediterranean and the Levant region in the eastern basin. AMJ  
<sup>119</sup> precipitation correlations are more uniform and strongly positive across nearly the entire  
<sup>120</sup> Mediterranean, suggesting that the summer season soil moisture variability, reflected in  
<sup>121</sup> the OWDA and the underlying tree growth, is driven primarily by spring precipitation  
<sup>122</sup> [c.f. *Touchan et al., 2014a*].

<sup>123</sup> Climate mode correlations with the CRU precipitation data or the OWDA scPDSI (Fig-  
<sup>124</sup> ure 3) are consistent in sign, but generally stronger in the precipitation data. The weaker  
<sup>125</sup> OWDA scPDSI correlations are expected for at least two reasons. First, these climate  
<sup>126</sup> modes reflect shifts in atmospheric circulation that have a direct impact on precipitation  
<sup>127</sup> by modulating, for example, storm track positions and moisture convergence. Circulation  
<sup>128</sup> impacts on the scPDSI will be by definition more indirect, as the scPDSI is computed  
<sup>129</sup> based on the anomalies of a variety of variables that influence soil moisture. Additionally,  
<sup>130</sup> up to year 1978, the scPDSI is reconstructed as a scaled linear function of the underlying  
<sup>131</sup> tree-ring proxies, which imparts additional uncertainties on the estimates of scPDSI.

<sup>132</sup> The influence of the NAO is strongest in winter and early spring (January–April;  
<sup>133</sup> JFMA). Positive phases of the NAO cause drying across the northern reaches of the

134 Mediterranean basin, from Spain and Morocco across to the Balkans and western Turkey,  
135 while favoring wetter conditions in coastal regions of Libya, Egypt, and the Levant. Con-  
136 sistent with both the instrumental observations [e.g. *Lamb et al.*, 1997; *Knippertz et al.*,  
137 2003] and the underlying controls on tree growth [*Touchan et al.*, 2008a, b; *Panayotov  
et al.*, 2010], the influence of the NAO in the OWDA is strongest in the far western part  
138 of the domain and the Balkans. The largest influence of the SCA pattern is during the  
139 winter (JFM), with positive phases increasing moisture across most of the basin. The SCA  
140 correlation with the OWDA is substantially weaker, consistent with previously analyses  
141 (Figure 2) demonstrating the much stronger connection between the OWDA and spring  
142 season, rather than winter, precipitation. Unlike the previous two modes, the influence of  
143 the EA is highest during the spring (AMJ), causing widespread drying across the basin  
144 with, notably, similar magnitude correlations with both precipitation and scPDSI.  
145

### 3.2. Drought Variability in the OWDA

146 Figure 4 shows OWDA scPDSI averaged over the Mediterranean domain and the fractional  
147 land area in drought ( $\text{scPDSI} \leq -1$ ) for each year from 1100–2012. Inter-annual variability  
148 (standard deviation) in the scPDSI is 0.54 standardized PDSI units and, on average, 29%  
149 of the basin experiences drought conditions in any given year. Highlighted are several  
150 example periods of persistent multi-year droughts and pluvials (Figure 4, grey bars).  
151 Noticeably absent are any extended multi-decadal (30-year or longer) ‘megadroughts’, a  
152 characteristic feature of North American drought variability during the Medieval Climate  
153 Anomaly (approximately before 1300 CE) [e.g., *Cook et al.*, 2010] and previously inferred  
154 from Moroccan tree-rings [*Esper et al.*, 2007].

The spatial expression of the six highlighted periods of widespread drought (and one pluvial) are shown in Figure 5. The most dramatic wet interval was a nearly two-decade long period from 1125–1142 CE, with sustained wet conditions in modern day Spain, Morocco, Algeria, Tunisia, Italy, the Balkans, and Turkey. This pluvial coincided with an extended period (1118–1179 CE) of low flows in the Upper Colorado River Basin (UCRB) in North America [the most persistent dry period in that region over the last millennium; *Meko et al.*, 2007], severe drought in the Sacramento River Basin [*Meko et al.*, 2012], and widespread drought across most of North America [*Cook et al.*, 2014]. This synchrony may suggest some large-scale persistent anomaly in atmospheric circulation across the Atlantic, possibly related to shifts in Atlantic sea surface temperatures [*Hu and Feng*, 2012]. Among the five highlighted persistent drought events, there is a tendency for simultaneous drought in the extreme western (Spain, Morocco, Algeria, Tunisia) and eastern (Balkans, Greece, Turkey) ends of the basin. This is somewhat contrary to previous analyses of other proxy records in the region, which have suggested instead a tendency for an antiphased dipole in hydroclimate variability between these two regions [e.g., *Roberts et al.*, 2012]. The basin-wide synchrony found in these example events is further confirmed by compositing all years when at least 40% or 50% of the basin is in drought (Figure 6). Here again, we observe the major poles of synchronous and severe drought during these years of widespread drought are centered over the opposite ends of the basin. There is, however, evidence for antiphasing in the eastern end of the basin, where there is a tendency for Libya, Egypt and the southern Levant to be wet or near normal when Greece and Anatolia are in drought. This meridional dipole structure bears some resemblance to the NAO correlation patterns with precipitation and scPDSI (Figure 3).

### 3.3. Spatial Synchrony

To further investigate the tendency for synchronous hydroclimate variability across the basin, we averaged scPDSI from the OWDA over three regions: the western Mediterranean (WestMED; 32°N–42°N, 10°W–0°E), the eastern Mediterranean (EastMED; 36°N–41°N, 20°E–37°E), and an area encompassing coastal Egypt, the southern Levant, and other areas of the Middle East (MidEast; 30°N–34°N, 33°E–47°E). The first two areas (WestMED and EastMED) correspond to approximately the same areas used in the analysis of *Roberts et al.* [2012]. Point-by-point correlations (Figure 7) between these three indices and the OWDA are strongly positive at the local level, as expected, decaying in magnitude outside of the averaging regions. For WestMED the correlations remain mostly positive, or near zero, across the entire basin. EastMED, however, shows strong negative correlations over Libya, Egypt, and the Levant while MidEast is negatively correlated with a large region surrounding the Black Sea. As with the drought composites (previous section), these results again suggest a strong tendency for meridional antiphasing in hydroclimate in the eastern Mediterranean Basin, with a pattern similar to what would be expected due to precipitation responses to variations in the NAO.

Spectral analyses of WestMED and EastMED show significant power in both series at high (inter-annual) and low (decadal to multidecadal) frequencies (Figure 8). Both have significant peaks at about 3–4 years, with EastMED additionally peaking at decadal frequencies and WestMED covering a broader range of multi-decadal bands. The two regions also overlap in their power at around 70 years, though EastMED is only marginally significant at the 90<sup>th</sup> percentile. A coherency spectra analysis between the two regional indices demonstrates highly significant coherence between the two regions over inter-annual and

200 decadal timescales (Figure 9). Notably, there is also a broad band of coherence between  
201 the two regions at multi-decadal and centennial timescales (30 to 130 years), despite no  
202 significant spectral peaks at wavelengths longer than  $\sim$ 75 years in either WestMED or  
203 EastMED. This may be due to overlaps in shared frequencies: both series have peaks at  
204 around 70-75 years, approximately the first harmonic of the 130 year coherence reflected  
205 in the coherency spectra. An analysis of the relative phasing for these spectral bands (not  
206 shown) indicates that the null hypothesis (that WestMED and EastMED are in phase)  
207 cannot be rejected at the  $p \leq 0.05$  significance level. These results are further confirmed  
208 by a cross-wavelet coherency analysis (Figure 10). These results show that EastMED and  
209 WestMED share significant variance in the decadal to centennial frequency bands for most  
210 of the analysis period and that these two series are primarily in phase (i.e., black arrows  
211 point to the right). Further, EastMED and MidEast have significant coherence at inter-  
212 annual to multidecadal frequencies, but are largely 180 degrees out of phase (i.e., blacks  
213 arrows are primarily pointing to 90 degrees to the left). These results indicate that, at  
214 least over the last millennium, there is a reasonably strong tendency for in-phase drought  
215 in the zonal direction across the Mediterranean, a notable contrast to the inferences made  
216 by *Roberts et al.* [2012]. Interestingly, given the association between the North Atlantic  
217 and western Mediterranean drought variability (Figure 3), there is no suggestion from the  
218 OWDA (Figure 9) that the NAO was in a persistent positive phase during the Medieval  
219 epoch. This is in contrast with the conclusions from *Esper et al.* [2007] and *Trouet et al.*  
220 [2009], but in agreement with a recent multiproxy reconstruction of the NAO by *Ortega*  
221 *et al.* [2015].

### 3.4. Recent Droughts

Recent decades have witnessed persistent, multi-year droughts in the Mediterranean that have spurred speculation that warming induced drying trends may have begun to emerge. In the OWDA, these droughts are not coherent across the Mediterranean basin but are instead highly localized in the WestMED region, Greece ( $36^{\circ}\text{N}$ – $43^{\circ}\text{N}$ ,  $19^{\circ}\text{E}$ – $26^{\circ}$ ), and the Levant ( $30^{\circ}\text{N}$ – $37^{\circ}\text{N}$ ,  $33^{\circ}\text{E}$ – $40^{\circ}\text{E}$ ) (Figure 11). Both WestMED and Greece experienced significant droughts in the 1980s and 1990s that have since ameliorated. The driest period in the Levant began in 1998 and has been generally ongoing since. Here, we attempt to place these most recent drought events within the context of OWDA drought variability for the last 900 years (Figure 12).

Over the last 30 years (1980–2012), we identify major periods of persistent drought in all three of these regions: 1980–2009 (WestMED), 1984–2002 (Greece), and 1998–2012 (Levant) (Figure 13, black dots). For each region, we then calculate the driest previous interval of the same length (Figure 13, grey dots). For both of these intervals, we estimate sampling uncertainties (the whiskers) using a resampling procedure where we randomly draw years from each interval with replacement, recalculating the mean scPDSI 10,000 times. The whiskers represent the 25<sup>th</sup> and 75<sup>th</sup> percentiles of these resampled means.

In general agreement with *Touchan et al.* [2008a], the recent persistent droughts in WestMED and Greece qualify as the most severe on the record. In both regions, however, there is substantial overlap in the uncertainties, and the recent droughts are not significantly drier (Student's t-test and Wilcoxon rank sum test,  $p > 0.10$ ) than the previous driest intervals. From this, we conclude that, while severe, recent droughts in the

<sup>243</sup> WestMED region and Greece are not statistically separable from natural drought vari-  
<sup>244</sup> ability over the last 900 years.

<sup>245</sup> The magnitude of the recent Levant drought exceeds the magnitude of the driest  
<sup>246</sup> previous interval in the region. In the Levant, mean scPDSI for 1998–2012 is  $-1.52$ ,  
<sup>247</sup> compared to  $-1.1$  for 1205–1219, with non-overlapping confidence limits between the  
<sup>248</sup> two events. Despite this separation, 1998–2012 is not significantly drier than the pre-  
<sup>249</sup> vious driest period (One-Sided Student's t-test,  $p = 0.13$ ). This is likely due to the  
<sup>250</sup> leveraging of the mean scPDSI for 1998–2012 by several extremely dry years: 1999  
<sup>251</sup> (scPDSI=  $-3.25$ ), 2000 (scPDSI=  $-4.49$ , the driest single year in this region back to  
<sup>252</sup> 1100), 2008 (scPDSI=  $-2.80$ ), and 2012 (scPDSI=  $-2.72$ ). In 89% of our simulations,  
<sup>253</sup> however, the resampled mean scPDSI for 1998–2012 was drier than the resampled mean  
<sup>254</sup> for the previous driest interval, 1205–1219. We therefore conclude that it is likely that  
<sup>255</sup> 1998–2012 in the Levant was the driest 15-year period of the last 900 years, suggesting  
<sup>256</sup> the possible emergence of a greenhouse gas forced drying signal.

#### 4. Discussion and Conclusions

<sup>257</sup> Paleoclimate reconstructions provide better sampling of the full range and spectrum of  
<sup>258</sup> natural variability in the climate system, variability that is often not adequately captured  
<sup>259</sup> by the relatively short instrumental record. This knowledge is especially critical for identi-  
<sup>260</sup> fying decadal and multidecadal variability and for evaluating the extent to which anthro-  
<sup>261</sup> pogenic forcing may be influencing recent climate trends and events. But while a variety  
<sup>262</sup> of local reconstruction efforts have been previously undertaken for the Mediterranean,  
<sup>263</sup> field reconstructions provide an opportunity to understand natural and anthropogenic  
<sup>264</sup> patterns at broader spatial and extended temporal scales.

Our analysis of the OWDA shows significant decadal to multi-decadal variability in hydroclimate across the Mediterranean, with significant coherence between the western and eastern basin centers on multi-decadal to centennial time scales and meridional antiphasing in the eastern Mediterranean Basin. The dynamics driving these patterns are still uncertain, but the NAO or processes linked to the North Atlantic are likely to be a major contributor [Hurrell and Loon, 1997; Eshel and Farrell, 2000]. The NAO mode is negatively correlated with precipitation and scPDSI across most of the basin (Figure 2) and at the decadal scale is associated with same-sign wet season (boreal winter) precipitation anomalies from Morocco and the Iberian Peninsula through western and central Anatolia, with opposing anomalies in the Levant [Mariotti et al., 2002; Xoplaki et al., 2004]. And while there is a zonal dipole in the Mediterranean tree-ring response to precipitation, with a stronger winter response to the west and an increasing spring-summer signal in the east [Touchan et al., 2014a, b], at decadal timescales at least the summer scPDSI does appear to reflect the broad-scale forcing of precipitation anomalies associated with the NAO. This creates a basin-wide coherence between northwestern Africa, the Balkans, and western Anatolia (Figure 9) and opposite sign anomalies in the Levant during major Mediterranean drought and pluvial events (Figure 5–7).

Interestingly, this coherent decadal pattern is somewhat different than that observed for recent scPDSI trends (Figure 11–13), with the western Mediterranean and the Levant experiencing more substantial drying trends, and with mixed signs over Anatolia. This suggests that North Atlantic ocean-atmosphere variability alone is unlikely to account for recent drought trends, and supports interpretations that greenhouse gas forcing has an important influence [Kelley et al., 2012; Seager et al., 2014; Kelley et al., 2015]. Although

288 some climate model simulations suggest recent NAO trends are outside the range of natural  
289 variability [Osborn, 2004; Kuzmina *et al.*, 2005], long control simulations can demonstrate  
290 unforced NAO variability similar to that seen in recent decades [Semenov *et al.*, 2008].  
291 Drying in the Levant is also likely influenced by recent trends toward a more positive EA  
292 pattern [Krichak *et al.*, 2002; Krichak and Alpert, 2005; Lim, 2014].

293 Our findings here suggest that, at least in the western Mediterranean and Greece,  
294 the recent severe decadal-scale dry conditions are not yet outside the range of natural  
295 variability, despite the influence of greenhouse gas forcing. In the Levant, however, we  
296 estimate that the last 15 years are likely the driest since the 12<sup>th</sup> century. Drought  
297 conditions here reduce water supply in the face of increasing demand, and create the  
298 potential for sociopolitical and economic disruption [e.g. Gleick, 2014; Kelley *et al.*, 2015],  
299 requiring a multidisciplinary research, management, and policy approach [Sohl and van  
300 Ginkel, 2014]. To that end, paleoclimate field reconstructions of drought can provide  
301 valuable information on the long-term and broad-scale context of recent events, especially  
302 how they fit within the context of natural climate variability.

303 **Acknowledgments.** Funding for Anchukaitis, Meko, and Touchan provided by grants  
304 from the NSF Paleo Perspectives on Climate Change (P2C2) program AGS-1103450, AGS-  
305 1103314, and AGS-1341066, with additional support from the NSF awards AGS-0317288  
306 (Earth System History), AGS-0758486, and AGS-0075956. Funding for the OWDA pro-  
307 vided to E. R. Cook by NOAA grant NA10OAR4310123. E.R. Cook and Anchukaitis  
308 are also supported by NSF AGS-1501856 and AGS-1502224. The Old World Drought  
309 Atlas data are available by request from the lead author (via email). This is Lamont  
310 contribution #.

## References

- 311 Akkemik, U., and A. Aras (2005), Reconstruction (1689-1994 AD) of April-August pre-  
312 cipitation in the southern part of central Turkey, *International Journal of Climatology*,  
313 25(4), 537–548, doi:10.1002/joc.1145.
- 314 Andreu, L., E. Gutiérrez, M. Macias, M. Ribas, O. Bosch, and J. J. Camarero (2007),  
315 Climate increases regional tree-growth variability in Iberian pine forests, *Global Change  
316 Biology*, 13(4), 804–815, doi:DOI:10.1111/j.1365-2486.2007.01322.x.
- 317 Barnston, A. G., and R. E. Livezey (1987), Classification, Seasonality and Persistence  
318 of Low-Frequency Atmospheric Circulation Patterns, *Monthly Weather Review*, 115(6),  
319 1083–1126, doi:10.1175/1520-0493(1987)115<1083:CSAPOL>2.0.CO;2.
- 320 Bueh, C., and H. Nakamura (2007), Scandinavian pattern and its climatic impact,  
321 *Quarterly Journal of the Royal Meteorological Society*, 133(629), 2117–2131, doi:  
322 DOI:10.1002/qj.173.
- 323 Büntgen, U., D. Frank, V. Trouet, and J. Esper (2010), Diverse climate sensitivity  
324 of Mediterranean tree-ring width and density, *Trees*, 24(2), 261–273, doi:10.1007/  
325 s00468-009-0396-y.
- 326 Chave, A. D., D. J. Thomson, and M. E. Ander (1987), On the robust estimation of  
327 power spectra, coherences, and transfer functions, *Journal of Geophysical Research:  
328 Atmospheres*, 92(B1), 633, doi:10.1029/jb092ib01p00633.
- 329 Chbouki, N., C. W. Stockton, and D. Myers (1995), Spatio-temporal patterns of drought  
330 in Morocco, *International Journal of Climatology*, 15, 187–205, doi:DOI:10.1002/joc.  
331 3370150205.

- 332 Cleveland, W. S., and S. J. Devlin (1988), Locally Weighted Regression: An Approach to  
333 Regression Analysis by Local Fitting, *Journal of the American Statistical Association*,  
334 83(403), 596, doi:10.2307/2289282.
- 335 Collins, M., R. Knutti, J. Arblaster, J.-L. Dufresne, T. Fichefet, P. Friedlingstein,  
336 X. Gao, W. Gutowski, T. Johns, G. Krinner, M. Shongwe, C. Tebaldi, A. Weaver,  
337 and M. Wehner (2013), Long-term climate change: Projections, commitments and ir-  
338 reversibility, in *Climate Change 2013: The Physical Science Basis. Contribution of*  
339 *Working Group I to the Fifth Assessment Report of the Intergovernmental Panel on*  
340 *Climate Change*, edited by T. Stocker, D. Qin, G.-K. Plattner, M. Tignor, S. Allen,  
341 J. Boschung, A. Nauels, Y. Xia, V. Bex, and P. Midgley, pp. 1029–1136, Cam-  
342 bridge University Press, Cambridge, United Kingdom and New York, NY, USA, doi:  
343 10.1017/CBO9781107415324.024.
- 344 Cook, B. I., J. E. Smerdon, R. Seager, and E. R. Cook (2014), Pan-Continental Droughts  
345 in North America over the Last Millennium, *Journal of Climate*, 27(1), 383–397, doi:  
346 10.1175/JCLI-D-13-00100.1.
- 347 Cook, E. R., D. M. Meko, D. W. Stahle, and M. K. Cleaveland (1999), Drought re-  
348 constructions for the continental United States, *Journal of Climate*, 12(4), 1145–1162,  
349 doi:[http://dx.doi.org/10.1175/1520-0442\(1999\)012<1145:DRFTCU>2.0.CO;2](http://dx.doi.org/10.1175/1520-0442(1999)012<1145:DRFTCU>2.0.CO;2).
- 350 Cook, E. R., R. Seager, R. R. Heim Jr, R. S. Vose, C. Herweijer, and C. Woodhouse  
351 (2010), Megadroughts in North America: placing IPCC projections of hydroclimatic  
352 change in a long-term palaeoclimate context, *Journal of Quaternary Science*, 25(1),  
353 48–61, doi:10.1002/jqs.1303.

- 354 Cook, E. R., P. J. Krusic, K. J. Anchukaitis, B. M. Buckley, T. Nakatsuka, and  
355 M. Sano (2013), Tree-ring reconstructed summer temperature anomalies for tem-  
356 perate East Asia since 800 C.E., *Climate Dynamics*, 41(11-12), 2957–2972, doi:  
357 10.1007/s00382-012-1611-x.
- 358 Cook, E. R., R. Seager, Y. Kushnir, K. R. Briffa, U. Büntgen, D. Frank, P. J. Krusic,  
359 et al. (in revision), Old World Droughts and Pluvials During the Common Era, *Science*  
360 *Advances*.
- 361 Czaja, A., and J. Marshall (2001), Observations of atmosphere-ocean coupling in the  
362 north atlantic, *Q.J Royal Met. Soc.*, 127(576), 1893–1916, doi:10.1002/qj.49712757603.
- 363 Eshel, G., and B. F. Farrell (2000), Mechanisms of eastern Mediterranean rainfall vari-  
364 ability, *Journal of the Atmospheric Sciences*, 57(19), 3219–3232.
- 365 Esper, J., D. Frank, U. Büntgen, A. Verstege, J. Luterbacher, and E. Xoplaki (2007), Long-  
366 term drought severity variations in Morocco, *Geophysical Research Letters*, 34(17),  
367 L17702, doi:10.1029/2007GL030844.
- 368 García-Ruiz, J. M., J. I. López-Moreno, S. M. Vicente-Serrano, T. Lasanta-Martínez, and  
369 S. Beguería (2011), Mediterranean water resources in a global change scenario, *Earth-  
370 Science Reviews*, 105(3–4), 121 – 139, doi:[http://dx.doi.org/10.1016/j.earscirev.2011.  
371 01.006](http://dx.doi.org/10.1016/j.earscirev.2011.01.006).
- 372 Giorgi, F., and P. Lionello (2008), Climate change projections for the Mediterranean  
373 region, *Global and Planetary Change*, 63(2–3), 90 – 104, doi:[http://dx.doi.org/10.1016/  
374 j.gloplacha.2007.09.005](http://dx.doi.org/10.1016/j.gloplacha.2007.09.005), mediterranean climate: trends, variability and change.
- 375 Gleick, P. H. (2014), Water, Drought, Climate Change, and Conflict in Syria, *Weather,  
376 Climate, and Society*, 6(3), 331–340, doi:10.1175/WCAS-D-13-00059.1.

- 377 Glueck, M. F., and C. W. Stockton (2001), Reconstruction of the North Atlantic Os-  
378 cillation, 1429–1983, *International Journal of Climatology*, 21, 1453–1465, doi:DOI:  
379 10.1002/joc.684.
- 380 Guttman, N. B. (1998), Comparing the Palmer Drought Index and the Standardized  
381 Precipitation Index, *Journal of the American Water Resources Association*, 34, 113–  
382 121, doi:10.1111/j.1752-1688.1998.tb05964.x.
- 383 Harris, I., P. D. Jones, T. J. Osborn, and D. H. Lister (2014), Updated high-resolution  
384 grids of monthly climatic observations –the CRU TS3.10 Dataset, *International Journal  
385 of Climatology*, 34(3), 623–642, doi:10.1002/joc.3711.
- 386 Held, I. M., and B. J. Soden (2006), Robust Responses of the Hydrological Cycle to  
387 Global Warming, *Journal of Climate*, 19(21), 5686–5699, doi:[http://dx.doi.org/10.  
388 1175/JCLI3990.1](http://dx.doi.org/10.1175/JCLI3990.1).
- 389 Hoerling, M., J. Eischeid, J. Perlwitz, X. Quan, T. Zhang, and P. Pegion (2012), On the  
390 Increased Frequency of Mediterranean Drought, *Journal of Climate*, 25(6), 2146–2161,  
391 doi:10.1175/JCLI-D-11-00296.1.
- 392 Hu, Q., and S. Feng (2012), AMO- and ENSO-Driven Summertime Circulation and Pre-  
393 cipitation Variations in North America, *Journal of Climate*, 25(19), 6477–6495, doi:  
394 10.1175/JCLI-D-11-00520.1.
- 395 Hurrell, J. W. (1995), Decadal Trends in the North Atlantic Oscillation: Regional Tem-  
396 peratures and Precipitation, *Science*, 269(5224), 676–679, doi:10.1126/science.269.5224.  
397 676.
- 398 Hurrell, J. W., and H. V. Loon (1997), Decadal Variations in Climate Associated with  
399 the North Atlantic Oscillation, in *Climatic Change at High Elevation Sites*, pp. 69–94,

- 400 Springer Netherlands, doi:10.1007/978-94-015-8905-5\_4.
- 401 Huybers, P. (2004), Comments on ‘coupling of the hemispheres in observations and sim-  
402 ulations of glacial climate change’ by a. schmittner, o.a. saenko, and a.j. weaver’, *Qua-*  
403 *ternary Science Reviews*, 23(1-2), 207–210, doi:10.1016/j.quascirev.2003.08.001.
- 404 Iglesias, A., L. Garrote, F. Flores, and M. Moneo (2007), Challenges to Manage the  
405 Risk of Water Scarcity and Climate Change in the Mediterranean, *Water Resources*  
406 *Management*, 21(5), 775–788, doi:10.1007/s11269-006-9111-6.
- 407 Jex, C. N., A. Baker, J. M. Eden, W. J. Eastwood, I. J. Fairchild, M. J. Leng, L. Thomas,  
408 and H. J. Sloane (2011), A 500 yr speleothem-derived reconstruction of late autumn–  
409 winter precipitation, northeast Turkey, *Quaternary Research*, 75(3), 399–405, doi:  
410 DOI:10.1016/j.yqres.2011.01.005.
- 411 Jones, M. D., C. N. Roberts, M. J. Leng, and M. Türkeş (2006), A high-resolution late  
412 Holocene lake isotope record from Turkey and links to North Atlantic and monsoon  
413 climate, *Geology*, 34(5), 361–364, doi:doi:10.1130/G22407.1.
- 414 Kelley, C., M. Ting, R. Seager, and Y. Kushnir (2012), The relative contributions  
415 of radiative forcing and internal climate variability to the late 20th Century win-  
416 ter drying of the Mediterranean region, *Climate Dynamics*, 38(9-10), 2001–2015, doi:  
417 10.1007/s00382-011-1221-z.
- 418 Kelley, C. P., S. Mohtadi, M. A. Cane, R. Seager, and Y. Kushnir (2015), Climate change  
419 in the Fertile Crescent and implications of the recent Syrian drought, *Proceedings of the*  
420 *National Academy of Sciences*, 112(11), 3241–3246, doi:10.1073/pnas.1421533112.
- 421 Knippertz, P., M. Christoph, and P. Speth (2003), Long-term precipitation variability  
422 in Morocco and the link to the large-scale circulation in recent and future climates,

- 423      Meteorology and Atmospheric Physics, 83(1), 67–88, doi:10.1007/s00703-002-0561-y.
- 424      Köse, N., U. Akkemik, H. N. Dalfes, and M. S. Özeren (2011), Tree-ring reconstructions  
425      of May–June precipitation for western Anatolia, *Quaternary Research*, 75(3), 438–450,  
426      doi:10.1016/j.yqres.2010.12.005.
- 427      Krichak, S., P. Kishcha, and P. Alpert (2002), Decadal trends of main Eurasian oscilla-  
428      tions and the Eastern Mediterranean precipitation, *Theoretical and Applied Climatology*,  
429      72(3-4), 209–220.
- 430      Krichak, S. O., and P. Alpert (2005), Decadal trends in the east Atlantic–west Russia  
431      pattern and Mediterranean precipitation, *International Journal of Climatology*, 25(2),  
432      183–192, doi:10.1002/joc.1124.
- 433      Kuzmina, S. I., L. Bengtsson, O. M. Johannessen, H. Drange, L. P. Bobylev, and M. W.  
434      Miles (2005), The North Atlantic Oscillation and greenhouse-gas forcing, *Geophysical*  
435      *Research Letters*, 32(4), doi:10.1029/2004gl021064.
- 436      Lamb, P. J., , M. E. Hamly, and D. H. Portis (1997), North Atlantic Oscillation, *Geo*  
437      *Observateur*, 7, 103–113.
- 438      Lim, Y.-K. (2014), The East Atlantic/West Russia (EA/WR) teleconnection in the North  
439      Atlantic: climate impact and relation to Rossby wave propagation, *Climate Dynamics*,  
440      doi:10.1007/s00382-014-2381-4.
- 441      Mann, M. E., and J. M. Lees (1996), Robust estimation of background noise and signal de-  
442      tection in climatic time series, *Clim. Change*, 33(3), 409–445, doi:10.1007/BF00142586.
- 443      Maraun, D., and J. Kurths (2004), Cross wavelet analysis: significance testing and pitfalls,  
444      *Nonlinear Processes in Geophysics*, 11(4), 505–514, doi:10.5194/npg-11-505-2004.

- 445 Maraun, D., J. Kurths, and M. Holschneider (2007), Nonstationary Gaussian processes  
446 in wavelet domain: Synthesis, estimation, and significance testing, *Phys. Rev. E*, 75,  
447 016,707, doi:10.1103/PhysRevE.75.016707.
- 448 Mariotti, A., M. V. Struglia, N. Zeng, and K. Lau (2002), The hydrological cycle in the  
449 Mediterranean region and implications for the water budget of the Mediterranean Sea,  
450 *Journal of climate*, 15(13), 1674–1690, doi:[http://dx.doi.org/10.1175/1520-0442\(2002\)015<1674:THCITM>2.0.CO;2](http://dx.doi.org/10.1175/1520-0442(2002)015<1674:THCITM>2.0.CO;2).
- 451 Meko, D., C. Woodhouse, and K. Morino (2012), Dendrochronology and links to stream-  
452 flow, *Journal of Hydrology*, 412-413(0), 200 – 209, doi:<http://dx.doi.org/10.1016/j.jhydrol.2010.11.041>, hydrology Conference 2010.
- 453 Meko, D. M., C. A. Woodhouse, C. A. Baisan, T. Knight, J. J. Lukas, M. K. Hughes, and  
454 M. W. Salzer (2007), Medieval drought in the upper Colorado River Basin, *Geophysical  
455 Research Letters*, 34(10), 10,705–10,709, doi:10.1029/2007GL029988.
- 456 Moreno, A., A. Pérez, J. Frigola, V. Nieto-Moreno, M. Rodrigo-Gámiz, B. Martrat,  
457 P. González-Sampériz, M. Morellón, C. Martín-Puertas, J. P. Corella, et al. (2012),  
458 The Medieval Climate Anomaly in the Iberian Peninsula reconstructed from marine  
459 and lake records, *Quaternary Science Reviews*, 43, 16–32, doi:DOI:10.1016/j.quascirev.  
460 2012.04.007.
- 461 Nicault, A., S. Alleaume, S. Brewer, M. Carrer, P. Nola, and J. Guiot (2008), Medi-  
462 teranean drought fluctuation during the last 500 years based on tree-ring data, *Climate  
463 Dynamics*, 31(2-3), 227–245, doi:10.1007/s00382-007-0349-3.
- 464 Ortega, P., F. Lehner, D. Swingedouw, V. Masson-Delmotte, C. C. Raible, M. Casado,  
465 and P. Yiou (2015), A model-tested North Atlantic Oscillation reconstruction for the

- 468 past millennium, *Nature*, 523(7558), 71–74, doi:10.1038/nature14518.
- 469 Osborn, T. (2004), Simulating the winter North Atlantic Oscillation: the roles of inter-  
470 internal variability and greenhouse gas forcing, *Climate Dynamics*, 22(6-7), doi:10.1007/  
471 s00382-004-0405-1.
- 472 Palmer, W. C. (1965), Meteorological drought, *Tech. rep.*, US Weather Bureau, Wash-  
473 ton, DC.
- 474 Panayotov, M., P. Bebi, V. Trouet, and S. Yurukov (2010), Climate signal in tree-ring  
475 chronologies of Pinus peuce and Pinus heldreichii from the Pirin Mountains in Bulgaria,  
476 *Trees*, 24(3), 479–490, doi:10.1007/s00468-010-0416-y.
- 477 Roberts, N., A. Moreno, B. L. Valero-Garcés, J. P. Corella, M. Jones, S. Allcock, J. Wood-  
478 bridge, M. Morellón, J. Luterbacher, E. Xoplaki, et al. (2012), Palaeolimnological evi-  
479 dence for an east–west climate see-saw in the Mediterranean since AD 900, *Global and*  
480 *Planetary Change*, 84, 23–34, doi:DOI:10.1016/j.gloplacha.2011.11.002.
- 481 Seager, R., N. Naik, and G. A. Vecchi (2010), Thermodynamic and Dynamic Mechanisms  
482 for Large-Scale Changes in the Hydrological Cycle in Response to Global Warming,  
483 *Journal of Climate*, 23(17), 4651–4668, doi:10.1175/2010JCLI3655.1.
- 484 Seager, R., H. Liu, N. Henderson, I. Simpson, C. Kelley, T. Shaw, Y. Kushnir, and  
485 M. Ting (2014), Causes of Increasing Aridification of the Mediterranean Region in  
486 Response to Rising Greenhouse Gases, *Journal of Climate*, 27(12), 4655–4676, doi:  
487 10.1175/JCLI-D-13-00446.1.
- 488 Seim, A., K. Treydte, V. Trouet, D. Frank, P. Fonti, W. Tegel, M. Panayotov,  
489 L. Fernández-Donado, P. Krusic, and U. Büntgen (2014), Climate sensitivity of Mediter-  
490 ranean pine growth reveals distinct east–west dipole, *International Journal of Clima-*

- 491 *tology, Early View*, doi:10.1002/joc.4137.
- 492 Semenov, V. A., M. Latif, J. H. Jungclaus, and W. Park (2008), Is the observed NAO vari-  
493 ability during the instrumental record unusual?, *Geophysical Research Letters*, 35(11),  
494 doi:10.1029/2008gl033273.
- 495 Sohl, M., and M. van Ginkel (2014), Drought preparedness and drought mitigation in the  
496 developing world's drylands, *Weather and Climate Extremes*, 3, 62 – 66, doi:[http://dx.  
497 doi.org/10.1016/j.wace.2014.03.003](http://dx.doi.org/10.1016/j.wace.2014.03.003), high Level Meeting on National Drought Policy.
- 498 Sousa, P. M., R. M. Trigo, P. Aizpurua, R. Nieto, L. Gimeno, R. Garcia-Herrera, P. Li-  
499 onello, and M. Maugeri (2011), Trends and extremes of drought indices throughout the  
500 20th century in the Mediterranean, *Natural Hazards & Earth System Sciences*, 11(1),  
501 33 – 51, doi:doi:10.5194/nhess-11-33-2011.
- 502 Thomson, D. J. (1982), Spectrum estimation and harmonic analysis, *Proceedings of the  
503 IEEE*, 70, 1055–1096.
- 504 Touchan, R., G. M. Garfin, D. M. Meko, G. Funkhouser, N. Erkan, M. K. Hughes, and  
505 B. S. Wallin (2003), Preliminary reconstructions of spring precipitation in southwestern  
506 Turkey from tree-ring width, *International Journal of Climatology*, 23(2), 157–171, doi:  
507 DOI:10.1002/joc.850.
- 508 Touchan, R., E. Xoplaki, G. Funkhouser, J. Luterbacher, M. K. Hughes, N. Erkan,  
509 U. Akkemik, and J. Stephan (2005), Reconstructions of spring/summer precipitation for  
510 the Eastern Mediterranean from tree-ring widths and its connection to large-scale atmo-  
511 spheric circulation, *Climate Dynamics*, 25(1), 75–98, doi:10.1007/s00382-005-0016-5.
- 512 Touchan, R., K. J. Anchukaitis, D. M. Meko, S. Attalah, C. Baisan, and A. Aloui (2008a),  
513 Long term context for recent drought in northwestern Africa, *Geophysical Research*

- 514      Letters, 35(13), L13,705, doi:DOI:10.1029/2008GL034264.
- 515      Touchan, R., D. Meko, and A. Aloui (2008b), Precipitation reconstruction for North-  
516      western Tunisia from tree rings, *Journal of Arid Environments*, 72(10), 1887–1896,  
517      doi:10.1016/j.jaridenv.2008.05.010.
- 518      Touchan, R., K. J. Anchukaitis, D. M. Meko, M. Sabir, S. Attalah, and A. Aloui (2011),  
519      Spatiotemporal drought variability in northwestern Africa over the last nine centuries,  
520      *Climate Dynamics*, 37(1–2), 237–252, doi:10.1007/s00382-010-0804-4.
- 521      Touchan, R., K. J. Anchukaitis, V. V. Shishov, F. Sivrikaya, J. Attieh, M. Ketmen,  
522      J. Stephan, I. Mitsopoulos, A. Christou, and D. M. Meko (2014a), Spatial Patterns of  
523      eastern Mediterranean climate influence on tree growth, *The Holocene*, 24(4), 381–392,  
524      doi:10.1177/0959683613518594.
- 525      Touchan, R., D. M. Meko, and K. J. Anchukaitis (2014b), Dendroclimatology in the  
526      Eastern Mediterranean, *Tree-Ring Research*, *in press*.
- 527      Trouet, V., J. Esper, N. E. Graham, A. Baker, J. D. Scourse, and D. C. Frank (2009),  
528      Persistent Positive North Atlantic Oscillation Mode Dominated the Medieval Climate  
529      Anomaly, *Science*, 324(5923), 78–80, doi:10.1126/science.1166349.
- 530      van der Schrier, G., J. Barichivich, K. R. Briffa, and P. D. Jones (2013), A scPDSI-based  
531      global data set of dry and wet spells for 1901–2009, *Journal of Geophysical Research:*  
532      *Atmospheres*, doi:10.1002/jgrd.50355.
- 533      Vicente-Serrano, S. M., S. Beguería, J. I. López-Moreno, M. Angulo, and A. El Kenawy  
534      (2010), A new global 0.5 gridded dataset (1901–2006) of a multiscalar drought index:  
535      comparison with current drought index datasets based on the Palmer Drought Severity  
536      Index, *Journal of Hydrometeorology*, 11(4), 1033–1043, doi:<http://dx.doi.org/10.1175/>

537 2010JHM1224.1.

- 538 Wassenburg, J. A., A. Immenhauser, D. K. Richter, A. Niedermayr, S. Riehelmann,  
539 J. Fietzke, D. Scholz, K. P. Jochum, J. Fohlmeister, A. Schröder-Ritzrau, et al. (2013),  
540 Moroccan speleothem and tree ring records suggest a variable positive state of the North  
541 Atlantic Oscillation during the Medieval Warm Period, *Earth and Planetary Science  
Letters*, 375, 291–302, doi:DOI:10.1016/j.epsl.2013.05.048.
- 542 Xoplaki, E., J. González-Rouco, J. Luterbacher, and H. Wanner (2004), Wet season  
543 Mediterranean precipitation variability: influence of large-scale dynamics and trends,  
544 *Climate Dynamics*, 23(1), doi:10.1007/s00382-004-0422-0.
- 545 Xu, C.-Y., and V. P. Singh (2002), Cross Comparison of Empirical Equations for Cal-  
546 culating Potential Evapotranspiration with Data from Switzerland, *Water Resources  
Management*, 16(3), 197–219, doi:10.1023/A:1020282515975.

## Tree–Ring Chronologies

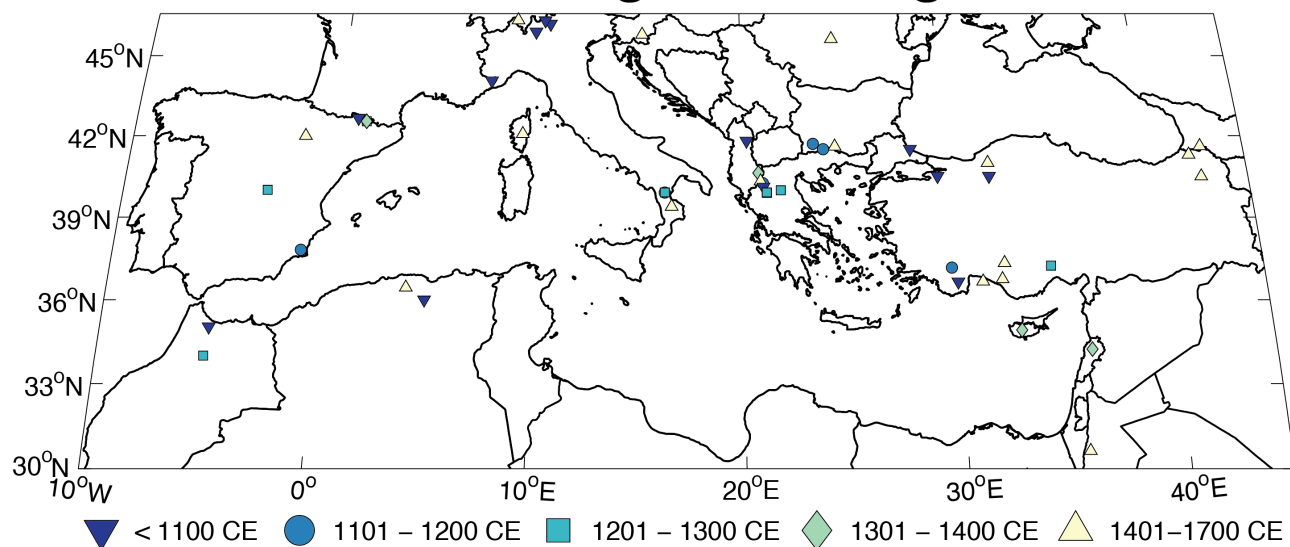


**Figure 1.** Locations of tree-ring chronologies used for the Mediterranean portion of the Old World Drought Atlas. Colors indicate the start dates of the various chronologies.

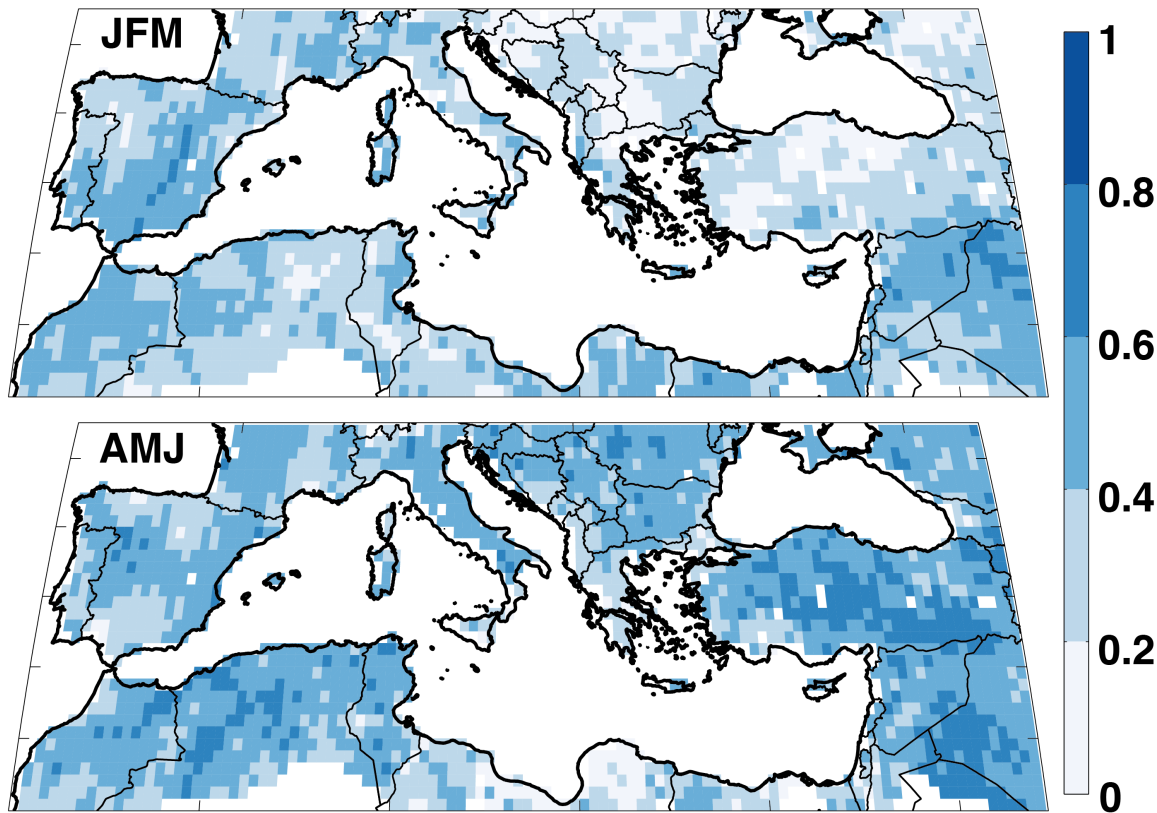


**Figure 2.** Point-by-point Spearman's rank correlation coefficients between CRU 3.21 precipitation totals (JFM and AMJ) and OWDA summer season (JJA) scPDSI. Correlations are calculated over the period 1950–2012 CE.

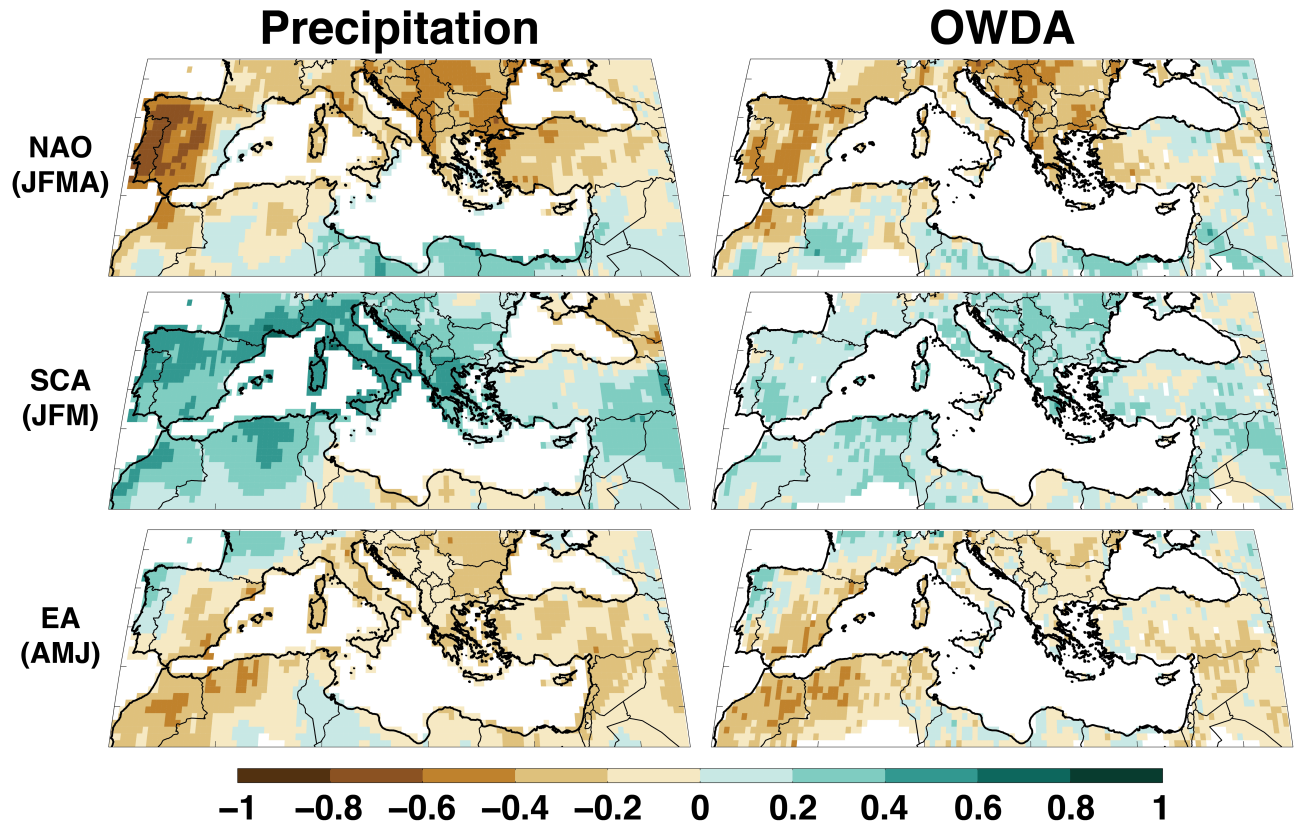


**Figure 3.** Spearman's rank correlation coefficients between the teleconnection indices (NAO, SCA, EA) and simultaneous season CRU 3.21 precipitation totals (left column) and OWDA summer season scPDSI (right column). Correlations are calculated over the period 1950–2012 CE.

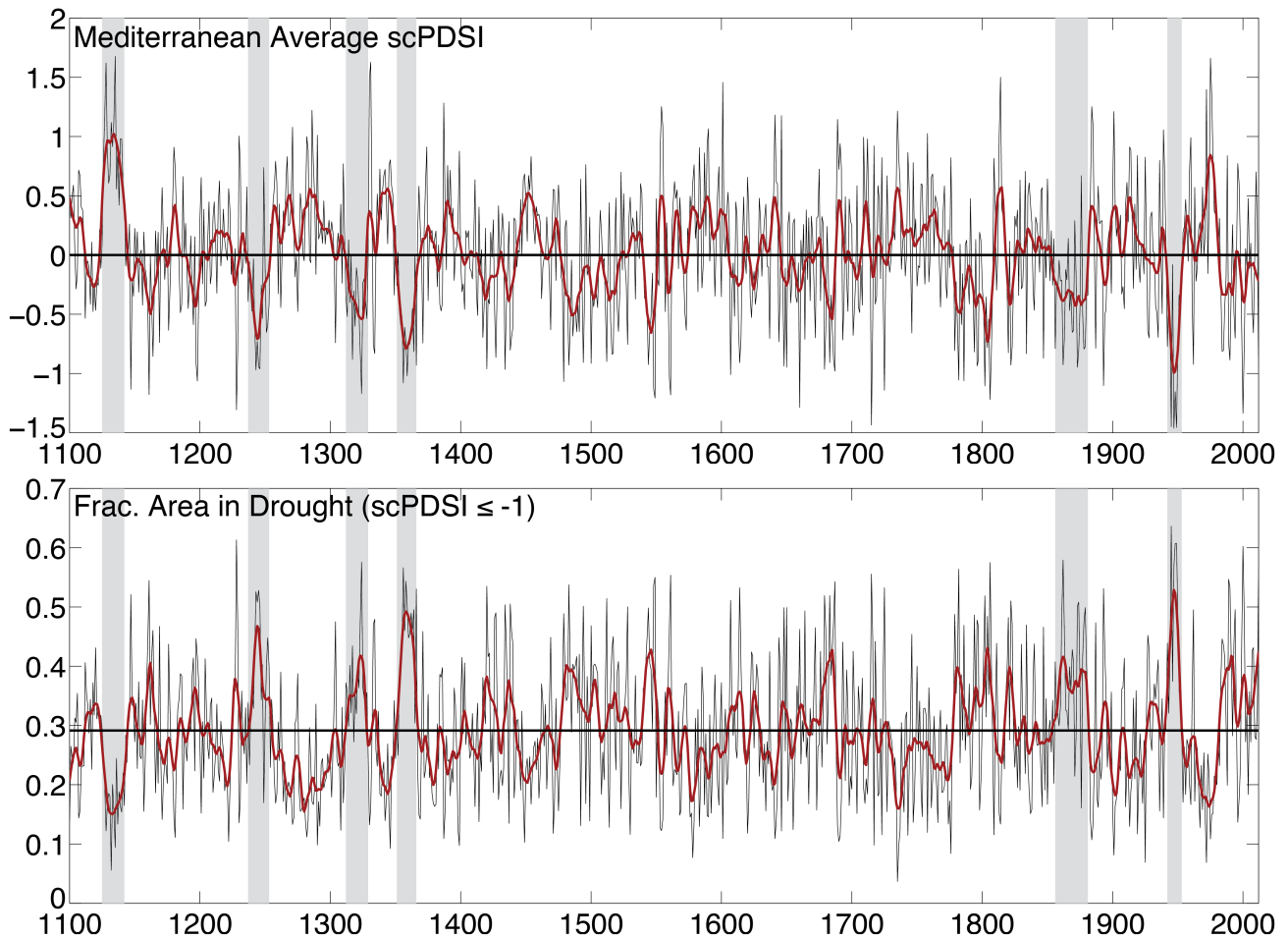


**Figure 4.** Area average scPDSI for the entire Mediterranean domain in the OWDA ( $30^{\circ}\text{N}$ – $47^{\circ}\text{N}$ ,  $10^{\circ}\text{W}$ – $45^{\circ}\text{E}$ ) (top) and percent land area in drought ( $\text{scPDSI} \leq -1$ ) (bottom) from 1100–2012 CE. Red curves are smoothed versions of the time series using a 10-year loess smooth. The horizontal line in the lower panel is the long-term average fractional area in drought from 1100–2012 CE (29%). Highlighted in grey are several example periods of persistent pan-basin drought and pluvial events (see Figure 5).

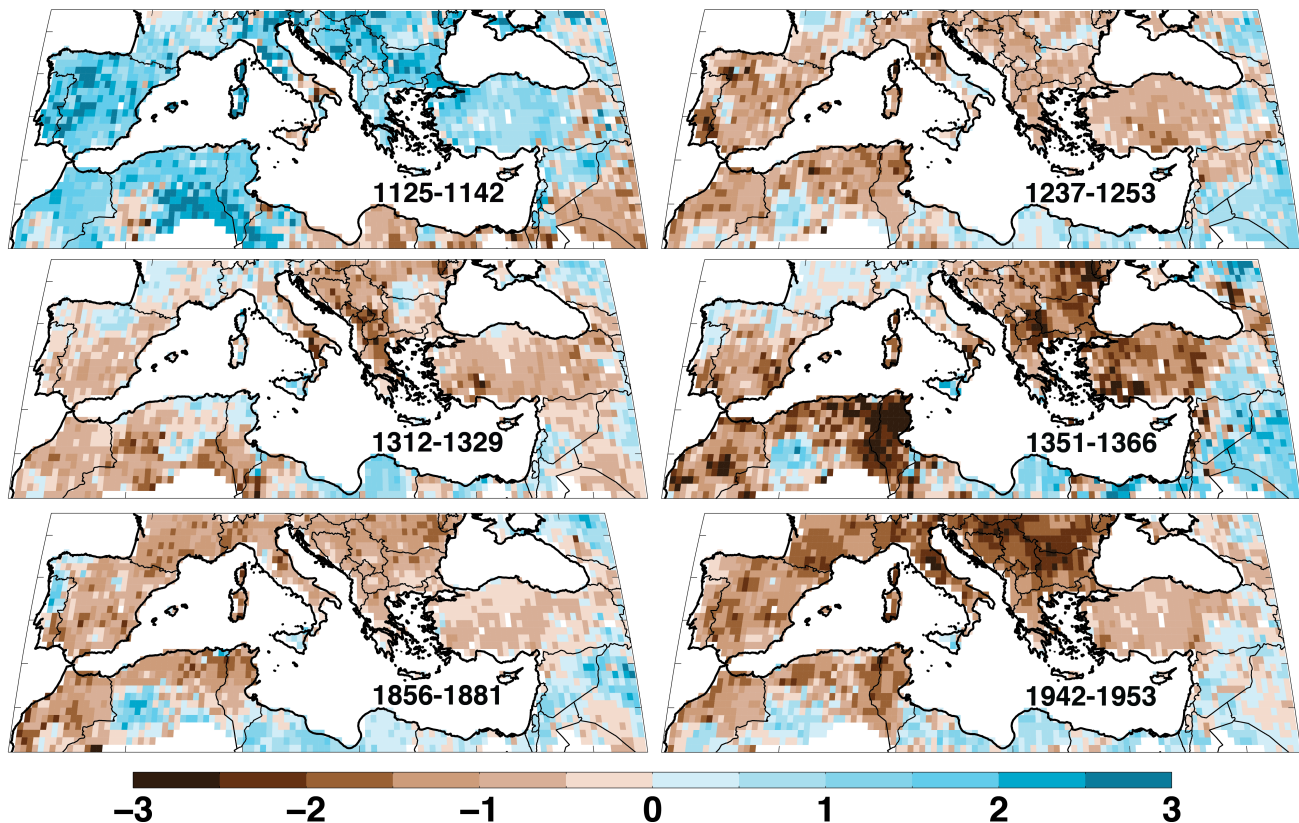


**Figure 5.** Multi-year average scPDSI for different pan-basin drought and pluvial events in the OWDA.

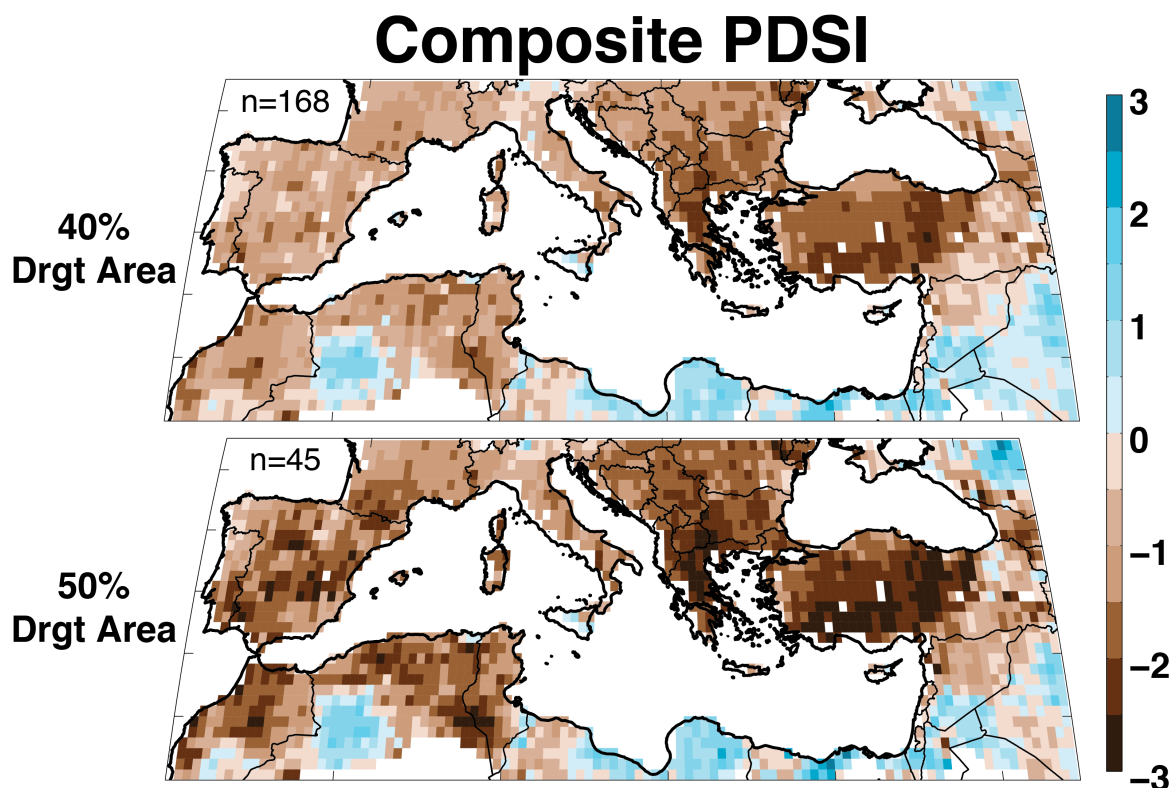


**Figure 6.** Composite average of Mediterranean drought events in the OWDA with a drought area ( $\text{scPDSI} \leq -1$ ) exceeding 40% ( $n = 168$  years) and 50% ( $n = 45$  years) of the total land area in the Mediterranean domain.

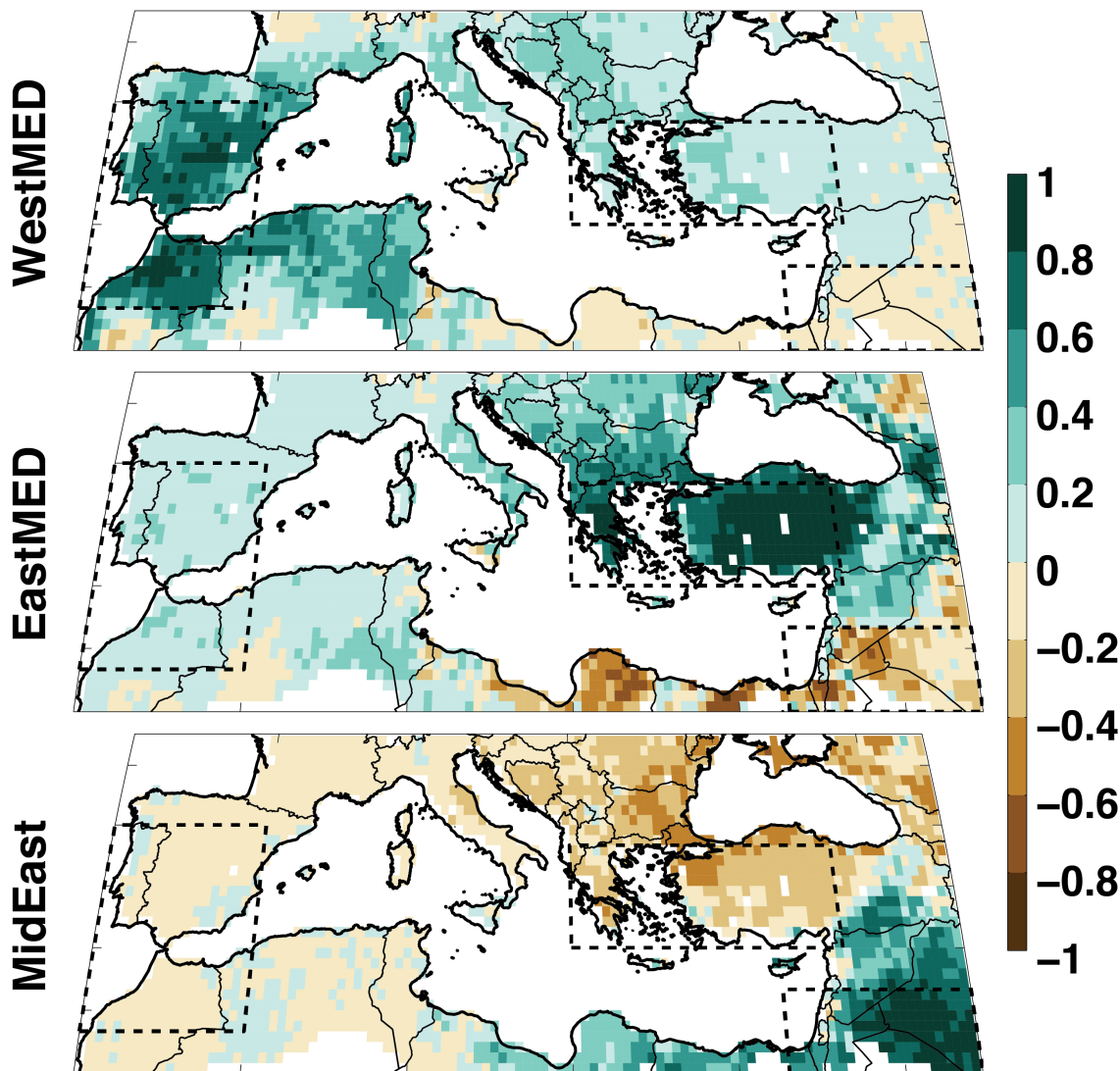


**Figure 7.** Point-by-point Spearman's rank correlations (1100–2012) between OWDA scPDSI and the Western Mediterranean (WestMED; 32°N–42°N, 10°W–0°), Eastern Mediterranean (EastMED; 36°N–41°N, 20°E–37°E), and Middle East (MidEast; 30°N–34°N, 33°E–47°E) regional average scPDSI time series.

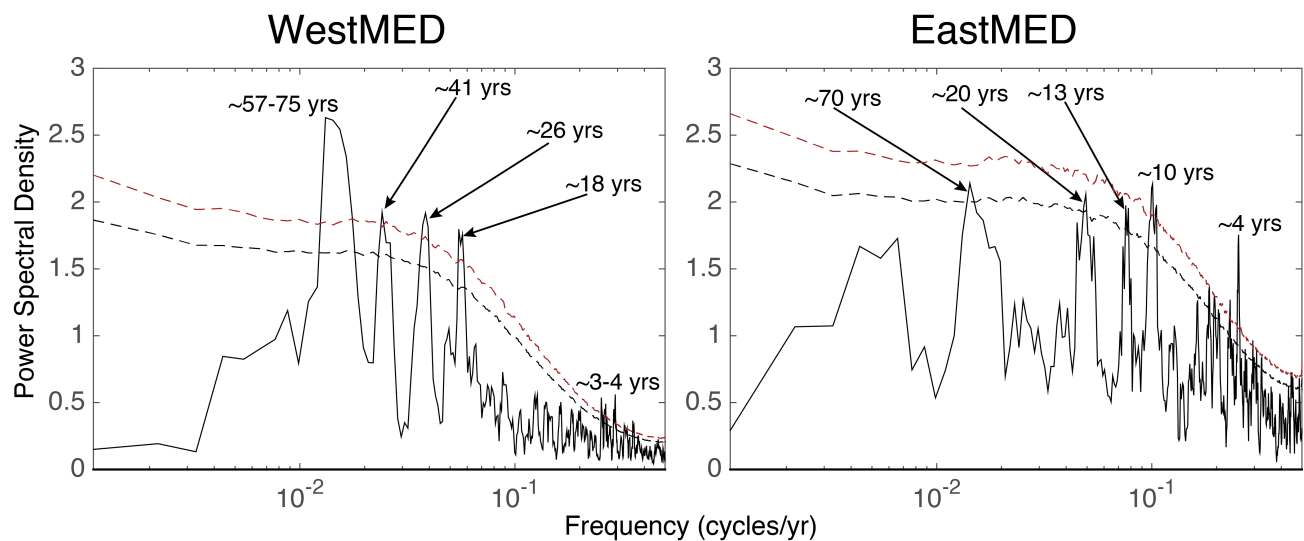


**Figure 8.** Power spectral density (Multi-taper Method, 3 tapers) for the WestMED and EastMED regional average scPDSI series. Red and black dashed lines are the 95<sup>th</sup> and 90<sup>th</sup> confidence limits, respectively, estimated from 10,000 AR(1) series generated from the original time series.

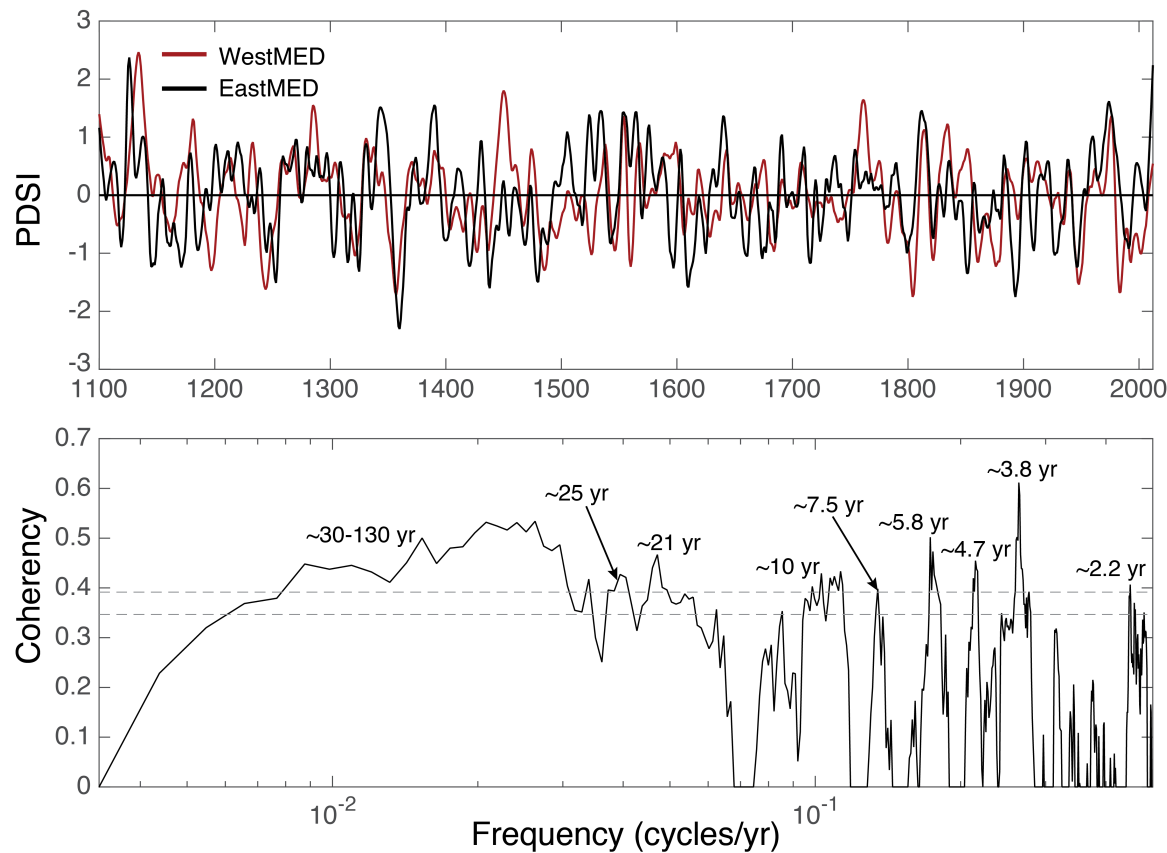


**Figure 9.** Smoothed versions (10-year loess smooth) of the WestMED and EastMED time series (top) and the coherency spectra between the two unsmoothed series (bottom).

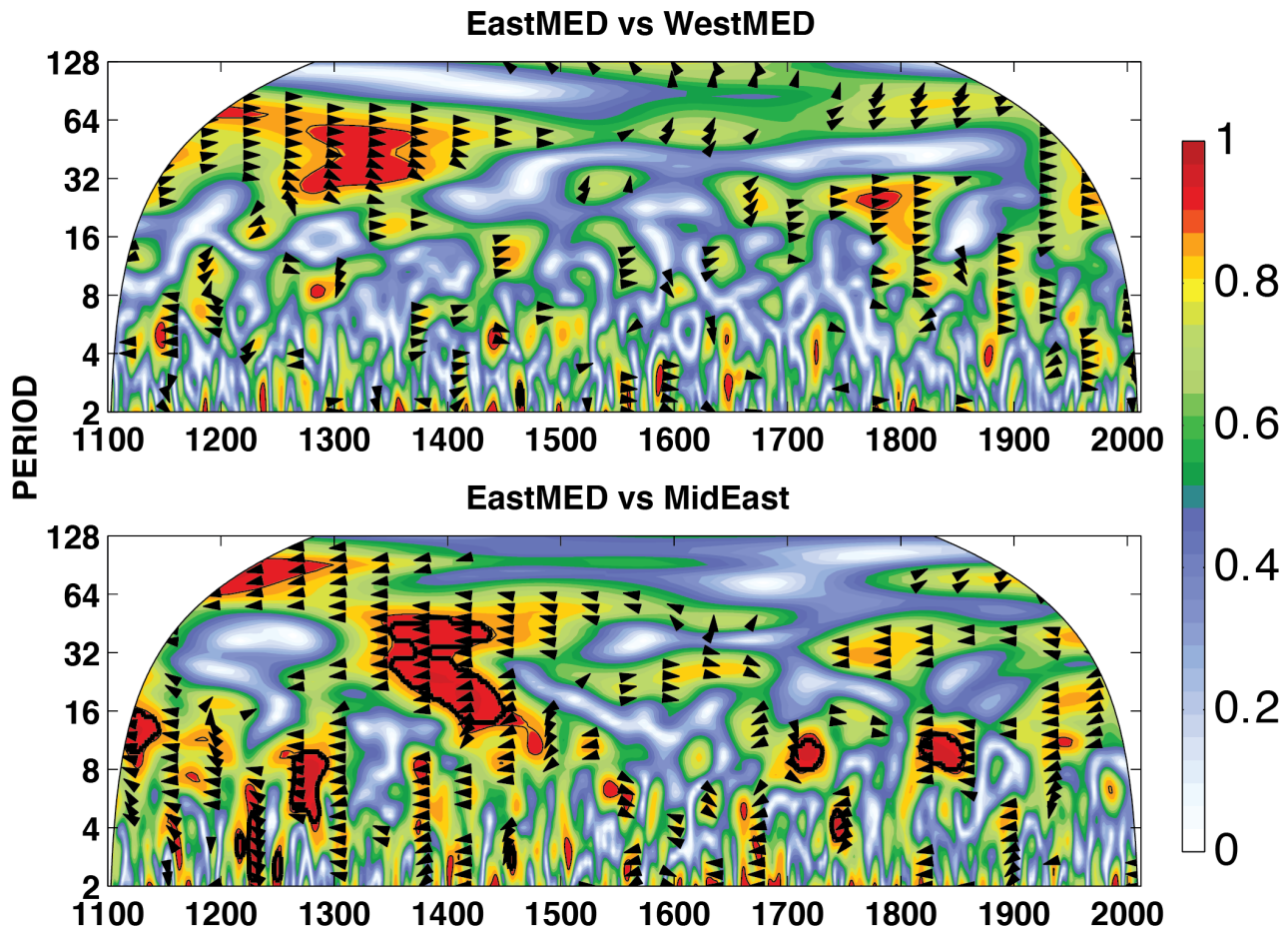


**Figure 10.** Squared wavelet coherence for EastMED versus WestMED (top) and EastMED versus MidEast (bottom). Black arrows pointing directly right indicate where the two time series have significant ( $p \leq 0.05$ ) shared variance and are in phase; black arrows pointed left indicate where the two series are  $180^\circ$  degrees out of phase.

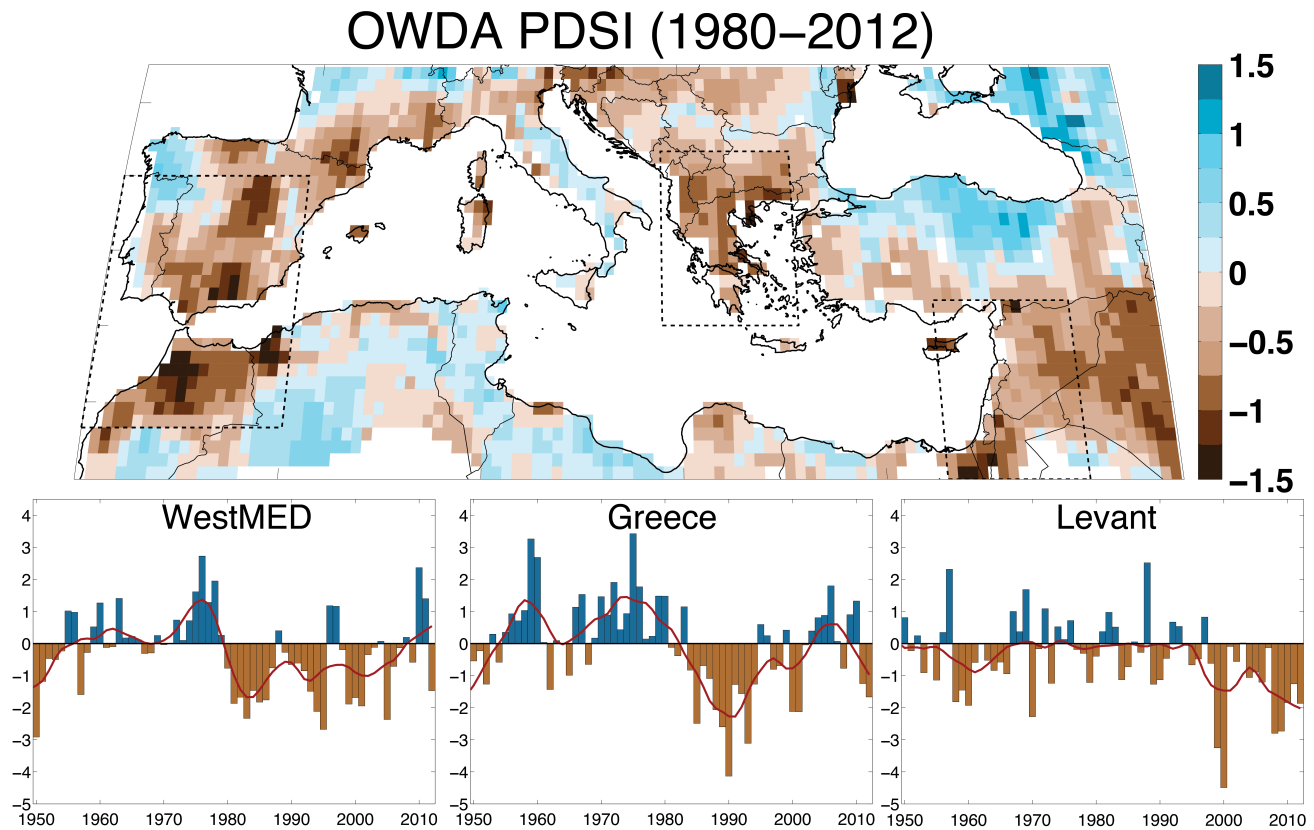


**Figure 11.** Multi-year average scPDSI for 1980–2012 (top) with regions of recent and persistent drought outlined in dashed black lines: WestMED ( $32^{\circ}\text{N}$ – $42^{\circ}\text{N}$ ,  $10^{\circ}\text{W}$ – $0^{\circ}$ ), Greece ( $36^{\circ}\text{N}$ – $43^{\circ}\text{N}$ ,  $19^{\circ}\text{E}$ – $26^{\circ}$ ), and the Levant ( $30^{\circ}\text{N}$ – $37^{\circ}\text{N}$ ,  $33^{\circ}\text{E}$ – $40^{\circ}\text{E}$ ). Also shown (bottom) are the regional average scPDSI time series from these regions for 1950–2012 (red line is a 10-year loess smoother).

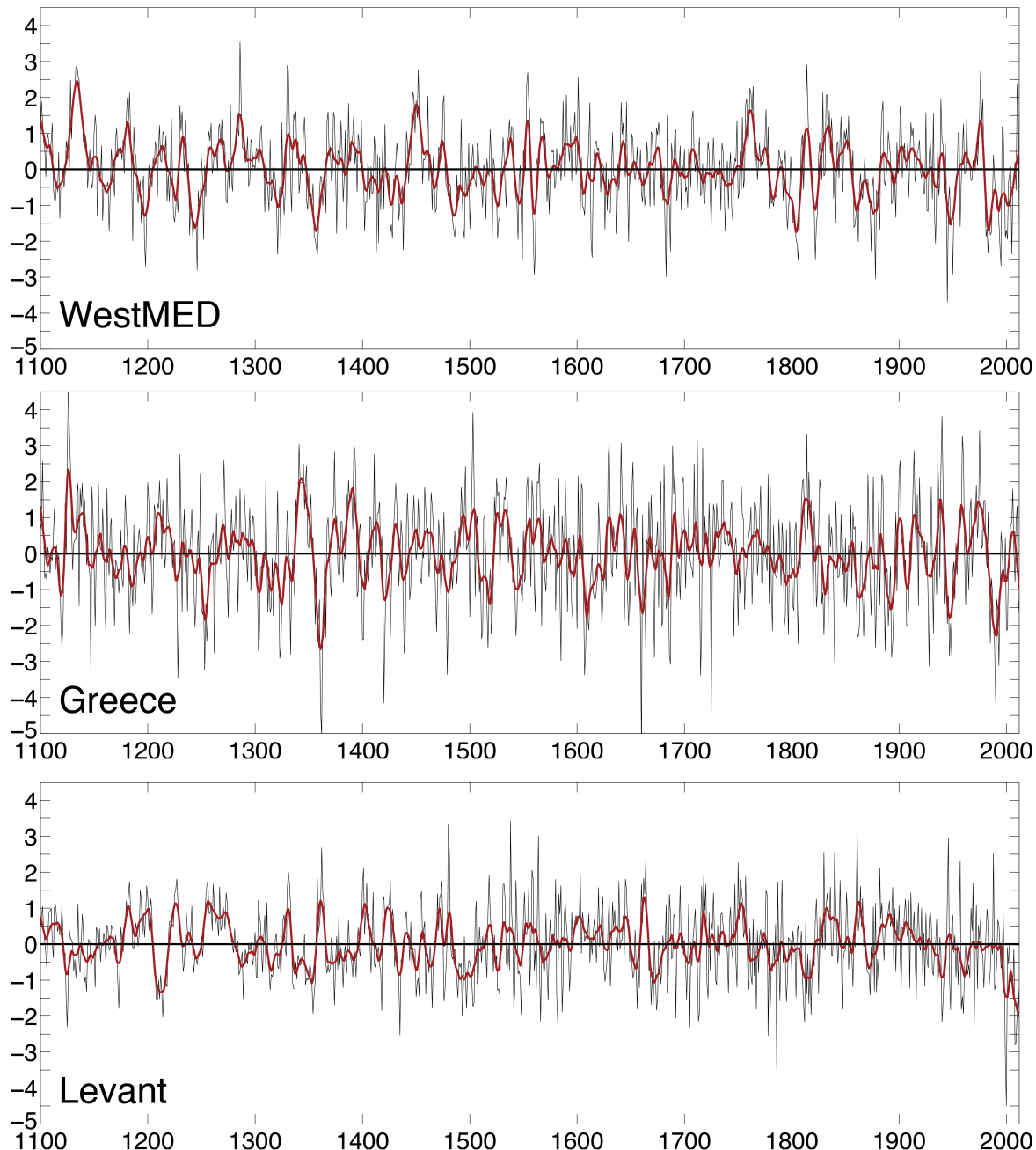


**Figure 12.** Re-centered (zero mean from 1100–2012 CE) time series for WestMED, Greece, and the Levant region. Red lines represent smoothed versions using a 10-year loess smoother.

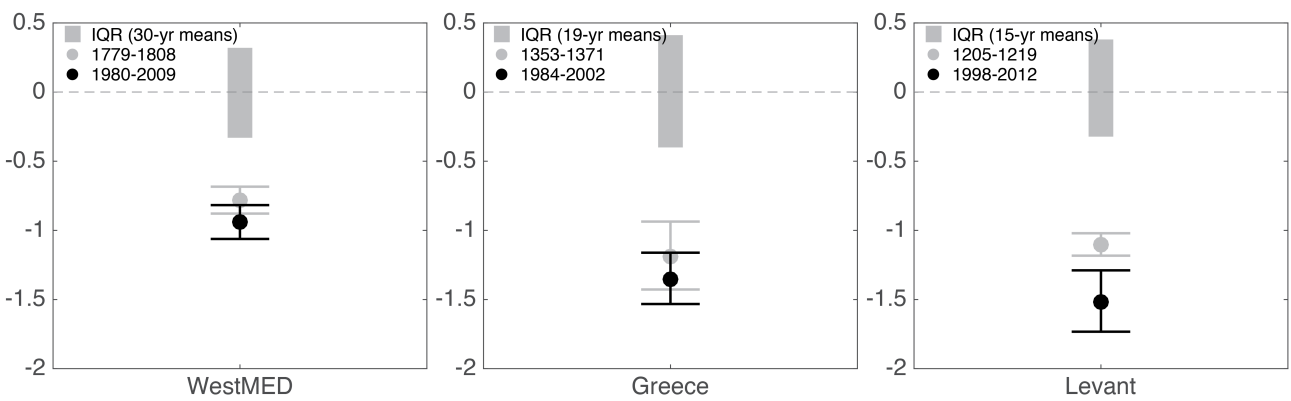


**Figure 13.** Comparisons between multi-year average re-centered scPDSI during recent decades (black dots) and driest previous periods of the same length in the OWDA from 1100–2012 CE. Grey bars are the interquartile range of mean PDSI for all such periods, grey dots represent the driest period prior to the recent decades, and black dots are the mean PDSI for the most recent drought. Whiskers are the 25<sup>th</sup> and 75<sup>th</sup> confidence limits for the dry events, estimated from 10,000 resamplings with replacement from scPDSI values during these intervals.